

Investigating the effect of Doxorubicin and Tetracaine in Sarcoplasmic Reticulum MG23 Calcium Leak



Luis Gil

lmcg1@st-andrews.ac.uk

Supervised by Dr. Samantha Pitt,
School of Medicine, University of St. Andrews, St. Andrews, KY16 9TF

Completed in fulfilment of the Laidlaw Research and Leadership Scholarship
August 2022

Introduction

Doxorubicin, and its implications in cardiotoxicity

Doxorubicin (DOX) is a powerful chemotherapy agent which has been used to treat a range of cancers since the 1960s¹. DOX is derived from the bacterium *Streptomyces peucetius* and thus comes under the class of anti-cancer drugs known as anthracyclines¹. One of its major mechanisms takes place during DNA replication during which it inhibits the enzyme topoisomerase II (TOP2)². TOP2 causes transient double strand breaks of the covalent disulphide bonds in DNA, enabling another piece of DNA to be inserted, relieving supercoils that can stop the process of DNA replication³. DOX can bind to TOP2 and intercalate in replicating DNA such that replication is unable to proceed and apoptosis, cell death, is triggered. Whilst having poor selectivity for cancer cells, DOX inhibits the isoform TOP2a, which is cell-cycle dependent and therefore more abundant in proliferating tumour cells than healthy cells in the body⁴.

Due to the lack of specificity in administration of DOX to specific tissues, many side effects can occur. These include fatigue, alopecia, nausea, vomiting, and notably cardiac toxicity¹. Cardiomyocytes have a more limited ability to regenerate than most tissues making them more susceptible to permanent remodelling⁵. Cardiotoxicity can affect patients either acutely or chronically. Acute cardiotoxicity is characterised by reversible myopericarditis, left ventricular dysfunction, or arrhythmias occurring 2-3 days after DOX infusion^{1,6}. Chronic cardiotoxicity is characterised by pericarditis and irreversible cardiomyopathy leading to congestive heart failure with reduced ejection fraction occurring. Symptoms usually manifest within 30 days of DOX administration but can occur 10-15 years after DOX treatment has finished⁶. The incidence of acute cardiotoxicity has been reported as more common than chronic cardiotoxicity, affecting 11% and 1.7% of patients respectively⁶. Currently there is no defined treatment available for patients with a diagnosis of DOX-induced cardiotoxicity⁶. This work aims to better understand the role of DOX in disrupting calcium homeostasis in the heart so that adjunct therapies may be designed in the future that could prevent the occurrence of such symptoms in cancer treatment patients.

The physiological roles of calcium in the heart: contraction and apoptosis

Calcium, in its cationic form Ca^{2+} , is crucial in several processes in the heart such as excitation-contraction coupling and the apoptotic pathway. The sarcoplasmic reticulum (SR) acts as a functional store of calcium within cardiomyocytes, enabling release and sequestration. Calsequestrin (CSQ) is the main protein that binds Ca^{2+} in the SR, serving as a storage and buffering protein that can reduce the number of free calcium cations and creating a steeper concentration gradient for Ca^{2+} removal into the SR, enabling heart relaxation⁷. In cardiomyocytes, the intracellular release of calcium to increase cytosolic Ca^{2+} concentration from approximately 100nM to 1 μ M is the key step in initiating each contraction⁸. The sequestration of this calcium back into the SR via sarco/endoplasmic reticulum Ca^{2+} -ATPase (SERCA), and some extrusion of Ca^{2+} from the cell is key for relaxation between heart beats. Calcium release occurs primarily via bulky Ryanodine Receptors (RYRs), predominantly RYR2 in heart cells⁸. The EF-hand domain of the protein

detects cytosolic Ca^{2+} concentrations before release so that; if SR stores are too low, less calcium is released and if SR stores are overloaded, spontaneous release, known as store overload induced calcium release (SOICR), occurs^{9,10}. There are many other calcium release channels that play a role in calcium dynamics within the heart such as inositol 1,4,5-trisphosphate receptors (IP_3Rs), however, for simplicity this work focuses on RYR2s and the newly discovered channel Mistugumin-23 (MG23)¹¹. MG23 is a small 23kDa voltage-dependent, cation-conducting channel permeable to both K^+ and Ca^{2+} , whose physiological function is unknown¹². It has been proposed that MG23 may act as a SR calcium leak channel that becomes exacerbated in disease states, and thus is relevant when examining the effect of DOX on cardiomyocytes¹³.

Calcium also plays a clear role in regulating apoptotic cell death as a second messenger¹⁴. Apoptosis can be understood as a part of healthy tissue homeostasis when cell removal and cell proliferation are in balance, but dysregulation of this process can be a feature of several pathological conditions such as neurodegenerative disorders, AIDS, and DOX-induced cardiotoxicity¹⁵.

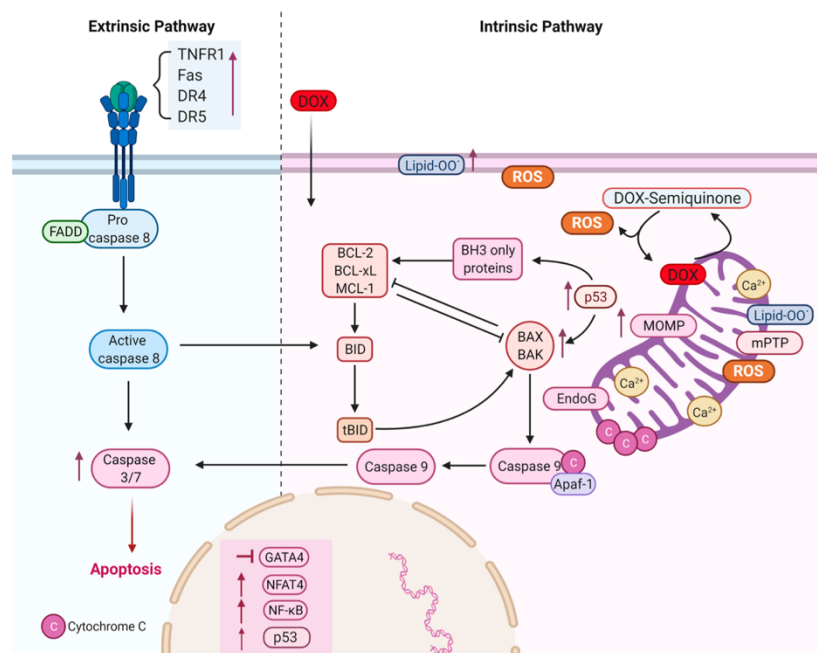


Figure 1 – A schematic of the intrinsic and extrinsic apoptotic pathways in a cell (unpublished data Pitt lab). Produced using Biorender.com

In simple terms, the apoptotic pathway in cells can be split into extrinsic (externally activated) and intrinsic (internally) activated routes. As shown in figure 1, both pathways eventually result in the production of Caspase 3 triggering apoptosis. Focussing on the intrinsic pathway, Cytochrome-C must be released from mitochondria via permeability transition pores (PTPs) and then bind with Apaf-1 to triggering the formation of large heptameric, wheel-like protein complexes called apoptosomes¹⁶. This enables the activation of caspase 9 and subsequently caspase 3. Many studies have proven reactive oxygen species and high cytosolic concentrations of calcium as potent endogenous activators of PTPs able

to induce apoptosis via the intrinsic pathway in cells¹⁷. Studies have linked MG23 overexpression to the cell death pathway in cells treated with topoisomerase II inhibitors, such as DOX¹⁸. An increased diastolic calcium leak via MG23 channels is sufficient to open PTPs, triggering apoptosis.

Diastolic calcium leak

In an idealised healthy heart model, strictly coordinated release and return of calcium from the SR is vital for contractions and relaxations, however, this is not quite the case in live cardiomyocytes. Diastolic calcium release that occurs outside of the period of excitation-contraction coupling is known collectively as calcium leak¹³. In normal physiology, the small amount of calcium leaked desensitises RYR2s and prevents the risk of cytosolic calcium stimulating aberrant diastolic contractions¹⁹. Whilst the molecular mechanism of the calcium leak is yet to be fully understood, it can be defined into a large visible RYR2-dependent leak and a smaller invisible RYR2-independent leak¹³. Visible and invisible refer to the ability of the calcium sparks to be seen using fluorescent Ca²⁺ tags and confocal microscopy²⁰. Tetracaine was used to attribute the larger visible leak to leaky RYR2s using whole cell fluorescence imaging²¹. The cause of the invisible leak remains disputed, but significant. Whilst the small leak that was uninhibited by tetracaine may seem inconsequential, it is thought to be upregulated in pathologies and thus also be a significant component in DOX-induced cardiotoxicity²¹. One suggested explanation for this is another leaky calcium channel, with MG23 being an encouraging cause of the leak. Data describing the biophysical characteristics of RYR2 channel gating showed substate gating at an amplitude of 1.7pA, matching the gating characteristics of MG23²². Later studies have proven that this could not be explained by RYR2 'substate gating', as they do not substate gate²³. We cannot be certain that MG23 is the cause of the small invisible leak, however, as the effects of Tetracaine on MG23 have not been explored.

Hypothesis, Aims, and Objectives

The hypothesis of this research project is that MG23 is a calcium leak channel that is implicated in heart cell calcium dysregulation and contributes to doxorubicin-induced cardiotoxicity patients.

The aims of the study are to (a) investigate the effects of doxorubicin and tetracaine on MG23 in isolated primary cardiomyocytes obtained from mice (b) at the single channel level determine if doxorubicin and tetracaine alter MG23 channel activity.

The objectives of the study are listed below:

1. Use electrophysiology techniques investigate the effects of tetracaine and doxorubicin on MG23 activity
2. Treat primary mice cardiomyocyte cells with doxorubicin and tetracaine to assess SR calcium store levels by addition of caffeine
3. Treat primary mice cardiomyocyte cells with doxorubicin and tetracaine to investigate MG23 expression

Methods

All chemicals and materials were sourced from Sigma, Aldrich UK unless otherwise stated. All chemicals were made up in Milli-Q de-ionised water (Milli-Q, Merck Millipore, UK).

Single Channel Electrophysiology

Sarcoplasmic Reticulum preparation

Solutions used were as follows:

Solution A (mM): 300 sucrose, 20 PIPES, pH made up to 7.2 with KOH

Solution B (mM): 0.5 MgCl₂, 0.5 EGTA, 0.5 CaCl₂, 25 PIPES, 2M KCl, pH made up to 7.2 with KOH

Solution C (mM): 5 HEPES, 0.4M sucrose, pH made up to 7.2 with Tris

Solution D (M): 0.4 KCl

250mM DTT

200mM PMSF

10%, 20%, 30%, and 40% Sucrose solutions dissolved in 20% Solution B

Method:

Previously established protocol as in (23) was followed²⁴.

Planar Lipid Bilayer

Solutions used were as follows:

3M LiCl

3M Choline Chloride

50mM Choline Chloride (mM): 50 Choline Chloride, 10 HEPES, 5 CaCl₂, made up to pH 7.2 with Tris

TrisHEPES (mM): 250 HEPES, made up to pH 7.2 with Tris

Calcium Glutamate (mM): 250 L-glutamic acid, 10 HEPES, made up to pH 7.2 with Ca(OH)₂

Method:

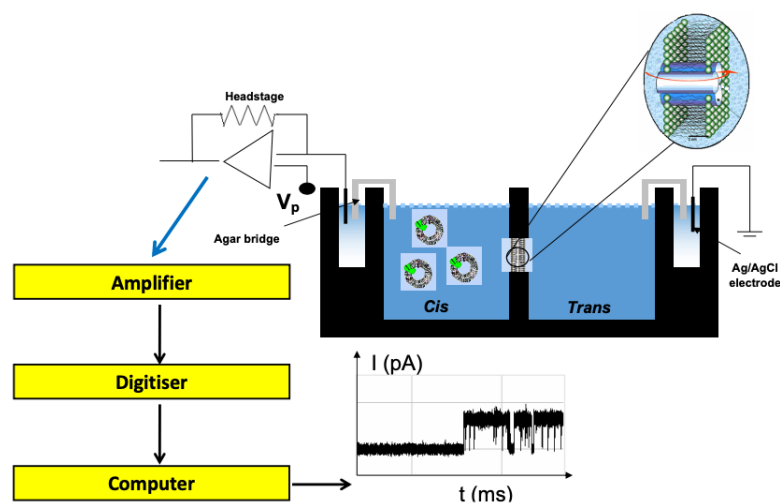


Figure 2 - Schematic of planar lipid bilayer rig apparatus used in the lab (unpublished data from Pitt lab)

Well established planar lipid bilayer protocol as in (24) was followed²⁵. Briefly following incorporation of isolated SR vesicles, solutions were reperused with TrisHEPES in the *cis* chamber and Calcium Glutamate in the *trans*, so that Ca^{2+} was the permeant ion. The *trans* chamber was held at ground, and the *cis* chamber was voltage-clamped at 0 mV. Current fluctuations were measured under voltage-clamp conditions using a BC-525C amplifier (Warner Instruments, Harvard). Channel recordings were low-pass filtered at 10 KHz with a four-pole Bessel filter, digitized at 100 KHz using a National Instruments acquisition interface (NIDAQ-MX, National Instruments, Austin, TX) and recorded on a computer hard drive using WinEDR software version 4.0.0 (John Dempster, University of Strathclyde, UK).

Current fluctuations were subsequently filtered at 800 Hz (-3 dB) using the low pass digital filter within WinEDR. All single channel analysis was carried out using WinEDR. Following 3 minutes of control recording at 0mV, 1mM tetracaine was added to the *cis* chamber and a subsequent 5 minutes of channel activity recorded. Solutions were then reperused to control conditions to test reversibility of tetracaine. 2.5 μM DOX was added to *cis* and channel fluctuations recorded for 3 minutes. Lastly, 2.5 μM DOX was added to *trans* and channel fluctuations recorded for a further 3 minutes.

Noise Analysis

Data was filtered at 800Hz low pass filter in WinEDR. Recordings were divided into records of 2048ms and variance analysis performed. Number of records and average mean direct current of the channel were then calculated using the noise analysis function in WinEDR v4.0.0. Mean direct current was calculated by plotting current fluctuations subdivided into N samples over time with the following equation:

$$I_{\text{mean}} = \frac{\sum_{i=1}^N I(i)}{N}$$

Where $I(i)$ is the i^{th} of N samples within the recording. Mean direct current was taken from recordings ≥ 1 minute and the calculated average was then plotted as a function of voltage.

Protein Expression Visualisation in Cardiomyocytes

Solutions

Ripa buffer (mM): 150 NaCl, 25 Tris-HCl, 1% sodium deoxycholate, 1% nonidet (NP-40), 0.1% SDS, 1 tablet in 10ml protease inhibitor (Complete mini EDTA-free, Roche, UK)

Collecting Lysates

All steps were completed at 4°C. Cultured cells were seeded and grown to confluency in a 10cm dish. Primary cells were plated in a 35mm petri dish. Cells were treated with 2.5 μM DOX, a clinical dose²⁶. Cells were then washed in cold PBS then lysed with RIPA buffer supplemented with EDTA-free protease inhibitor on ice. Cells were collected by scraping with a cell scraper into a 1.5ml microcentrifuge tube. Samples were kept on ice and sonicated with a Q-500 sonicator at 20% amplitude with 10 second pulses for 1 minute. They were then centrifuged at 10,000 rpm 4°C for 5 minutes to pellet debris. Supernatant was transferred into a fresh microcentrifuge tube and stored at -80°C.

Western Blot

Well established gel electrophoresis protocol was followed, using β -actin and Vinculin as loading controls²³.

Primary Antibodies:

For MG23: anti-TMEM109 in rabbit (Sigma, Aldrich, cat no. HP A011785)

For β -actin: anti- β -actin in rabbit (Cell Signalling Technology, USA, cat no. 49675)

For Vinculin: anti-vinculin monoclonal antibody (Sigma, Aldrich, cat no. MAB3574)

Analysis

Blots were imaged using ImageQuant LAS 4000.

Calcium Store Imaging of Cardiomyocytes

Solutions

Tyrode's solution (mM): 135 NaCl, 10 HEPES, 5 KCl, 5 Glucose, 5 sodium pyruvate, 1 MgCl₂, 0.33 NaH₂PO₄, pH 7.4 with NaOH

2 μ M Fluo-4 AM: 2 μ M Fluo-4 AM in Tyrode's solution

50 mM caffeine

Cell Treatment

Cardiomyocytes were treated with 2.5 μ M DOX and 1mM tetracaine were loaded into an 8 well plate for 24 hours to incubate. The wells were organised such that there were 4 controls (untreated), and 4 treated wells. At the 24 hour time point, cells were loaded with 2 μ M Fluo-4 for 20 minutes. Cells were then loaded in Ca²⁺ free tyrodes to deesterify.

Imaging

Cells were imaged for 3 minutes. At the 40 second mark, 10mM caffeine was added to induce calcium release from the SR. Images were taken every 0.5 seconds.

Analysis

Images were analysed using Fiji Image J software. Images were stacked, converted to 8-bit and brightness and contrast adjusted. Small oval areas of interest over surviving cells were selected, taking care to avoid nuclei. Colour density was measured for these points throughout the recording. Results were pasted into a Microsoft Excel table and normalised against the first image of each selected area to show change in fluorescence intensity over time, and a graph generated. The graphs were subsequently analysed to give the maximum peak response of calcium release after caffeine addition.

Results

Tetracaine reversibly modulates MG23 through cytosolic addition

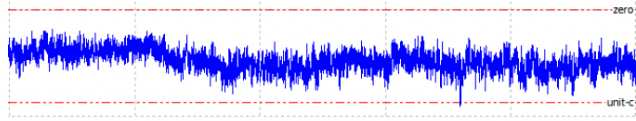
Tetracaine is a well established inhibitor of RYR channels. When quantifying the RYR2 dependent fraction of SR Calcium leak, tetracaine was used as a RYR2 blockade so that the reduction in calcium leak could be attributed to solely leaky RYR channels. However, a small RYR2-independent leak, uninhibited by tetracaine, was still present. The effect of tetracaine on MG23 is still not known, granting the possibility that the small 'invisible' RYR2-independent leak that occurred was due to this newly discovered channel.

As seen in figure 3, noise analysis showed that the mean direct current (D.C.) of MG23 decreased from 3.223pA to 2.646pA following addition of 1mM tetracaine. Looking at the graph, we can see that tetracaine had a weak inhibitory effect, taking around 3 minutes to reach maximum reduction in current. Following reperfusion and wash out of tetracaine from the system, mean D.C. increased to 3.454pA, similar to control conditions activity. Once again, the reversal of tetracaine's effect was not immediate, taking around 2 minutes to return to peak activity.

DOX increases MG23 activity via cytosolic addition

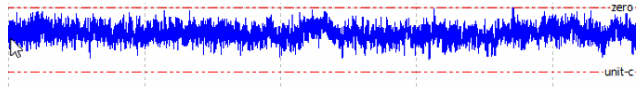
As shown in figure 3, 2.5 μ M DOX was then added to the *cis* chamber, causing mean D.C. to increase quickly to 4.831pA; a channel activity higher than in control conditions.

TrisHEPES (cis) / Ca²⁺ Glutamate (trans) at 0mv



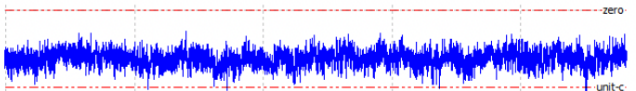
Mean D.C. = 3.223pA

TrisHEPES (cis) / Ca²⁺ Glutamate (trans) at 0mv
+ 1mM Tetracaine (cis)



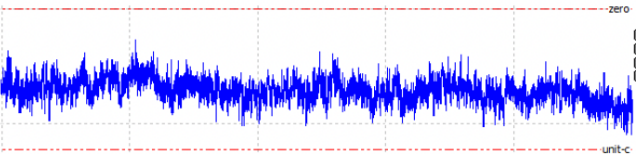
Mean D.C. = 2.646pA

TrisHEPES (cis) / Ca²⁺ Glutamate (trans) at 0mv
Following washout of Tetracaine



Mean D.C. = 3.454pA

TrisHEPES (cis) / Ca²⁺ Glutamate (trans) at 0mv
+2.5μM DOX (cis)



Mean D.C. = 4.831pA

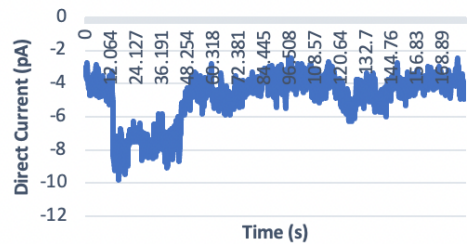
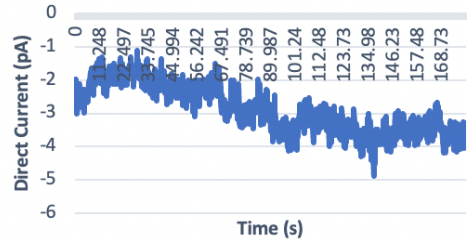
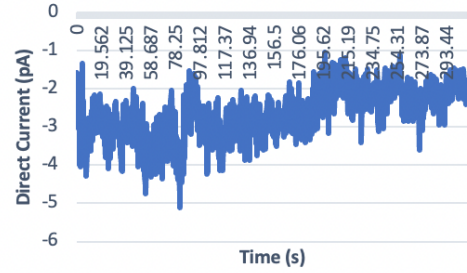
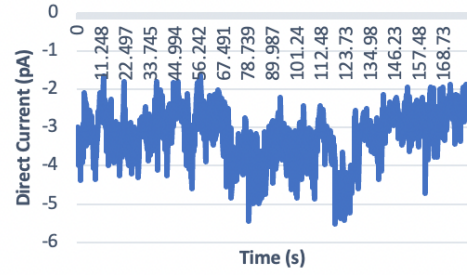


Figure 3 - Tetracaine and DOX addition to MG23 in an artificial bilayer. Each experiment shows a segment trace of the channel, the mean direct current (pA) of the channel throughout the recording, and a noise analysis graph. On the traces, zero corresponds to the closed state of the channel and unit-c corresponds to the open state. (n=2)

DOX depletes SR calcium stores by increasing MG23 Ca²⁺ leak

Primary cardiomyocyte cells were obtained from mice for this experiment by well established Langendorff-free cardiomyocyte isolation procedure²⁷. Cells were incubated with DOX and tetracaine for 24 hours. At the 24hr time point, the cells were then loaded with Fluo-4 AM, a fluorescent Ca²⁺ indicator, and imaged using a FITC filter cube – excitation 488nm. The emitted fluorescence was collected using a 500-550nm band-pass filter. All wells in the plate had very few surviving cardiomyocytes, suggesting most had died due to the DOX and tetracaine treatment. Here we show individual cell responses. Caffeine, a full activator of RYR2s, was added at 40 seconds into the recording to stimulate release of Ca²⁺ from the SR stores. Unfortunately no control cells survived treatment, however, to illustrate a typical response data from a different cardiomyocyte isolation has been taken (figure 6).

There was large variability in the cell responses following tetracaine and Dox treatment. As shown in figure 4, treated cells showed no robust response to caffeine addition at 40 seconds. Additionally, cells consistently produced a small gradual leak of calcium up to the point of caffeine addition.

Figure 6 shows the only treated cell that responded to the caffeine addition. Clearly, RYR2 channels were not blocked in this cell, however, a small potentially MG23 dependent leak still appears to be present initially.

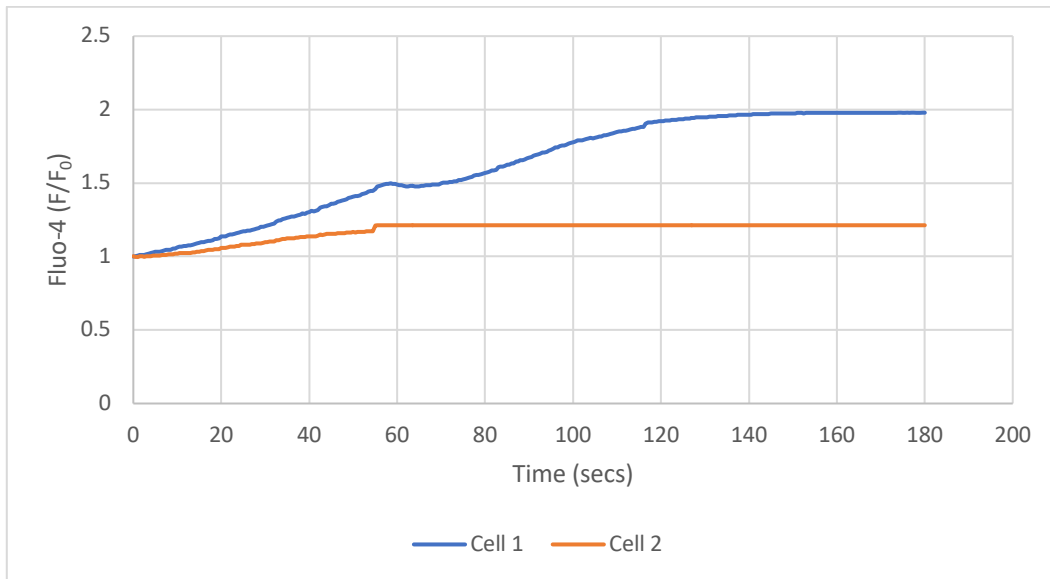


Figure 4 - Calcium imaging results for cells treated with 2.5 μ M DOX and 1mM Tetracaine. There is a small leak of calcium initially, no response to the caffeine, and then further leak that plateaus towards the end of the recording. (n=3)

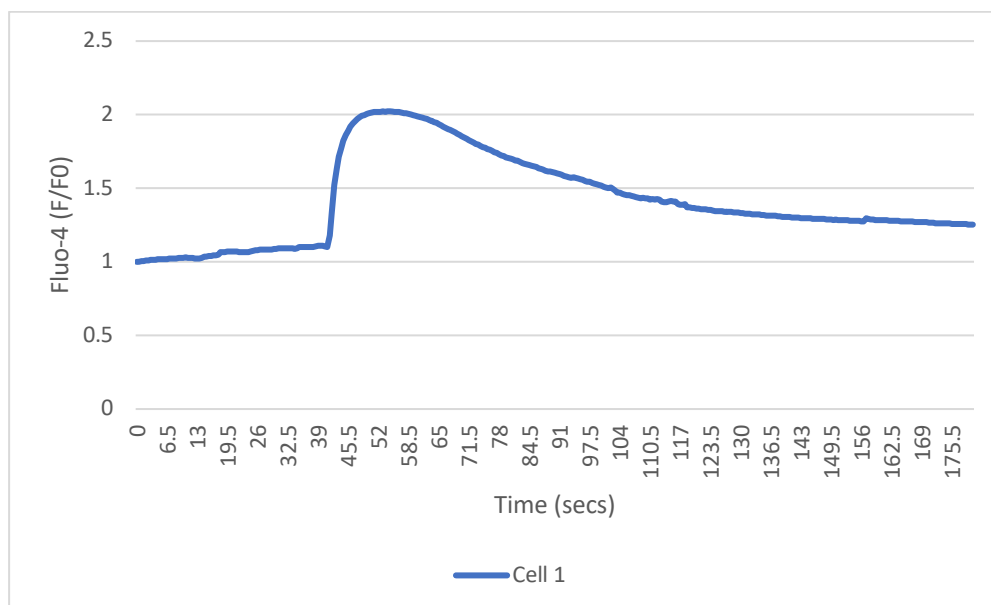


Figure 5 - Calcium imaging results for a cell treated with 2.5 μ M DOX and 1mM tetracaine. There is still a gradual calcium leak initially, but also a large peak in fluorescence at 40s due to caffeine addition.

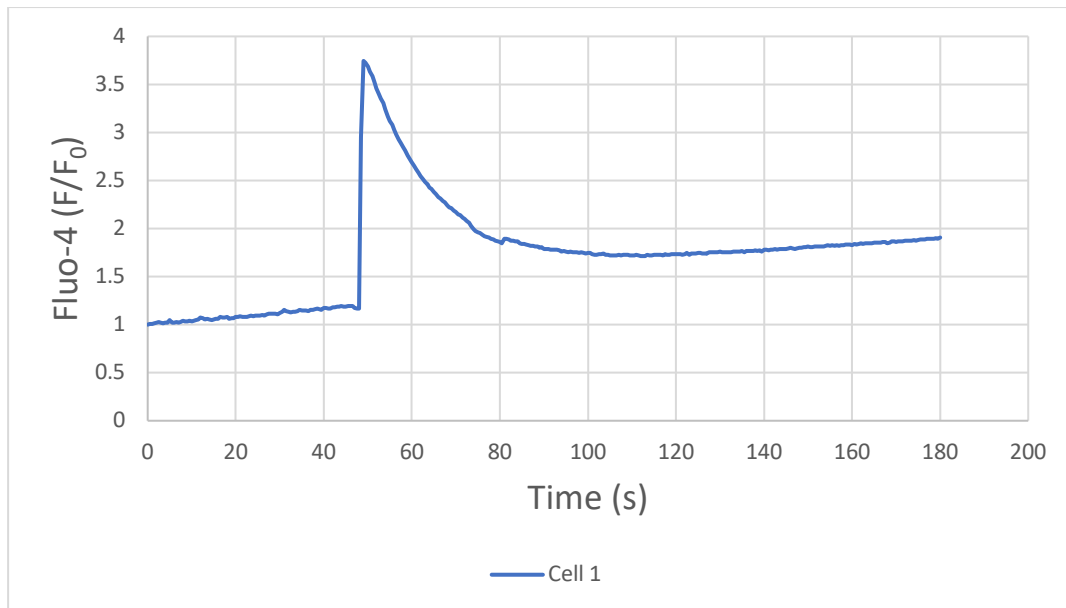


Figure 6 - A typical calcium response in untreated cardiomyocytes showing a much more instantaneous peak of calcium release (Unpublished data Pitt lab)

Protein Expression Visualisation following 24hr DOX treatment

With evidence showing that DOX could significantly increase MG23 activity via cytosolic addition of a clinical dose, the effect of DOX on MG23 protein expression was now necessary in cardiomyocytes. Some difficulties were encountered in running the western blot such as literature suggesting that DOX actually causes upregulation of vinculin, the loading control to which protein expression levels are usually normalised in the Pitt lab²⁸. Thus, anti- β -actin was used alongside the anti-vinculin as another loading control. After running the blot, the anti-MG23 antibody did not bind well due to degradation. The blot was stripped according to established protocol and new antibodies were applied, but this did not solve the problem either. Thus, a quantification of how MG23 protein expression changes with DOX treatment in primary cardiomyocytes could not be obtained.

Discussion and Conclusion

This study follows on from prior work done by the Pitt lab investigating the effect of DOX on MG23 and quantifying its role in cardiotoxicity. Research had been conducted using similar experiments on an immortalised rat ventricular cell line (H9C2 cells). Apart from unpublished data, the literature investigating the putative calcium channel MG23 and its role in calcium homeostasis as well as in pathophysiology is limited. Previous research, however, has indicated that calcium dysregulation is likely to be one of many contributors to DOX-induced cardiotoxicity^{29,30}.

MG23 activity is increased by luminal addition of DOX

In the single channel studies that we conducted; DOX activated MG23 when added to the *cis* chamber. However, as shown in figure 7 previous experiments describe luminal addition of DOX increasing the open probability of MG23 and the dwell time of openings. There is a possibility that DOX has a delayed effect, and thus the increased activation this data shows following *trans* addition of DOX is a result of it being added cytosolically earlier.

Furthermore, the solubility of DOX through lipid bilayers is still unknown, enabling the possibility that DOX could diffuse between chambers and not necessarily be activating MG23 from the face of the protein we added it directly to.

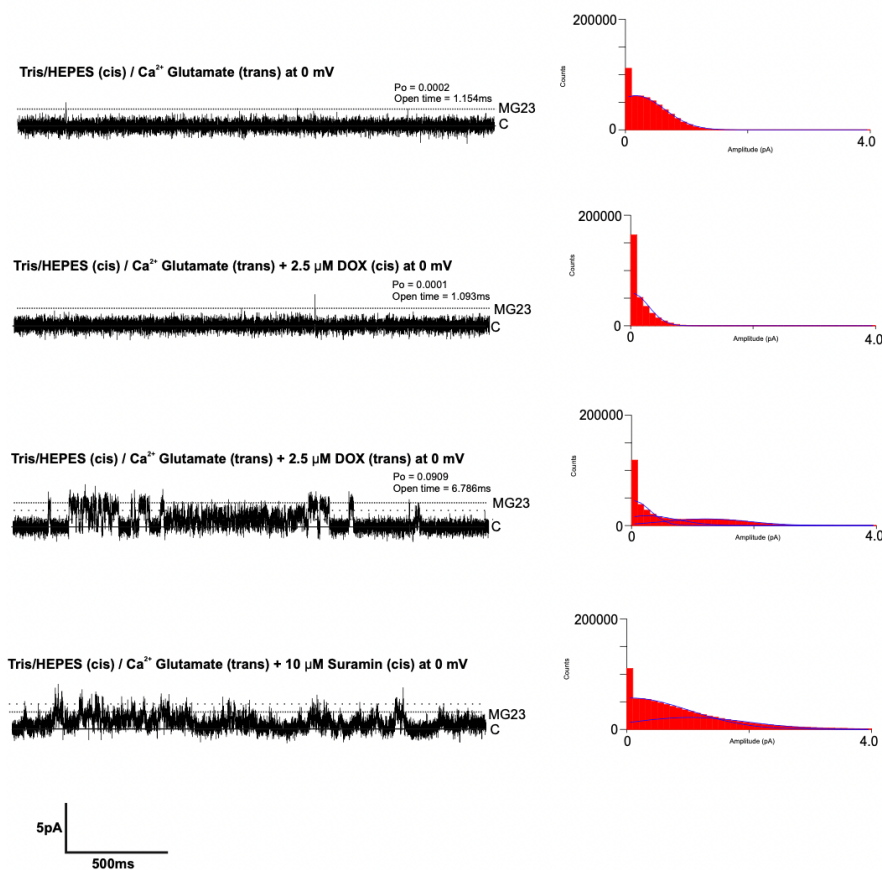


Figure 7 - Unpublished data from Pitt lab. A clinical dose of DOX increases activity of MG23 via luminal addition. (n=2)

All single channel experiments were done using native mouse protein preparations, containing both light and heavy SR fractions. Light SR tends to contain a greater proportion of MG23 channels, and heavy SR RYR2 channels. Whilst an n=2 in our single channel results certainly requires further confirmation of our findings, the use of native membranes aids in replicating the SR membrane inside a cell.

Unpublished data from the Pitt lab has also shown that DOX upregulates the expression of MG23 in H9C2 cells by 3-fold. Therefore, it was necessary to attempt the same experiment in mice cardiomyocytes to see if similar results would be produced. If the case is true that DOX can cause both increased expression and upregulation of activity of MG23, then MG23 has the potential to cause significant Ca²⁺ leak, and thus be a contributing factor in the cardiotoxicity associated with DOX treatment. Unfortunately, our protein expression data was inclusive.

Cytosolic addition of high 1mM tetracaine weakly modulates MG23 at single channel level

To provide further evidence that MG23 contributes to RyR2 independent SR Ca²⁺ leak, we investigated the direct effect of a high dose of tetracaine (1 mM) on MG23 channel activity. 1 mM tetracaine has been previously shown to completely close RyR2.

Our experiments shown in figure 3 show that tetracaine has a weak inhibitory effect on MG23 channel activity, but MG23 is still functional. This is exciting as this is the first direct evidence that MG23 could function as the RyR2 independent SR Ca²⁺ leak channel. The case may be that at 1mM, although tetracaine can slightly reduce MG23 activity, channel activity is still present. In whole cells there is likely to be a much lower tetracaine concentration present than the concentration we used in our single channel studies. Further investigation into the effects of varying concentrations of tetracaine at the micromolar level on MG23 are necessary to fully understand the pharmacology of this interaction in whole cells. In addition, future experiments would require more repeats of the experiment to ensure that all results are statistically significant. It may be the case that a goldilocks μ M concentration of tetracaine exists whereby we are able to entirely block RYR2 channels in whole cells, but have no effect on MG23, thus enabling us to visualise the 'invisible' RYR2-independent leak as described by Bers¹³.

More experiments are still needed to understand how tetracaine interacts with MG23, whether it is an allosteric modulator or a poor blocker. Investigation into channel conductance and single channel kinetics when tetracaine is bound could help provide a better description of the pharmacodynamics behind this.

SR Calcium store imaging

The results obtained from calcium store imaging unfortunately could not be compared to a control from the same cardiomyocyte isolation, due to all cells either dying or not responding in those wells. It is well known that primary cells are more sensitive and prone to death than immortalised cell lines, such as the H9C2 line. In our tetracaine and Dox treated cells we saw heterogeneity in our data. However, we consistently saw Ca²⁺ leakage from the cells. These data can be interpreted in multiple ways. (1): the cells visualised could simply have been dying cells and so were non-responsive to the caffeine treatment hence the lack of a calcium peak (2)Consistent with our single channel data showing DOX had a marked effect on MG23 channel activity, following 24hr treatment with DOX this could have caused significant SR store depletion through activation of MG23 , thus caffeine was unable to induce a large release of Ca²⁺ from the cells (3)the small leak visualised could be due to leaky RYR2 channels. We believe that the most convincing explanation for the results seen is explanation 2. Caffeine was unable to stimulate a calcium peak from the RYR2s. This may be due to tetracaine still blocking the channels. Additionally, DOX may have activated MG23 channels in the cell such that the leak seen is an increased MG23 responsible leak, reported to be 'invisible' by Bers¹³. Extrapolating from this, the plateau in fluorescence seen in figure 4 could be due to depletion of SR stores, and such there was no subsequent Ca²⁺ leak.

Future experiments investigating the combined effects of DOX and tetracaine on whole cells could do with a longer washout following the treatment period, to better understand the extent to which tetracaine is able to block RYR2 channels but not the putative MG23-dependent leak. A next step could be examining tetracaine half-life when using this technique to quantify the invisible RYR2-independent leak.

Potential Impact of the Study

This study is the first to establish that tetracaine does not fully shut MG23, and establishes the theories that MG23 was responsible for the RYR2-independent leak first described by Bers¹³. Furthermore, successful whole cell experiments investigating calcium store levels set a positive direction to visualise what was previously thought to be invisible, and to precisely quantify this leak in the future. If the MG23-dependent leak can be proven as a large proportion of the leak in DOX-treated cells, this more seriously implicates it in the pathophysiology behind DOX-induced cardiotoxicity, and stresses MG23 as a druggable target to treat patients suffering from cardiotoxicity.

Future research

Whilst various experiments have investigated the interactions between DOX and mouse MG23, the next steps of research must move on to the human model. There are some reported differences between mouse and human MG23 such as a cysteine residue in the transmembrane region of the protein, as shown in figure 8, that require exploration²⁵. Furthermore, properties of DOX such as its solubility through membranes and its exact crystal structure are yet to be obtained. The former is important as it could answer questions as to whether DOX can move between both chambers during planar lipid bilayer experiments, hence the confusion in cytosolic and luminal activation of MG23; the latter would aid in the specific identification of a DOX binding site on MG23. Furthermore, as MG23 is expressed throughout the body, not only in the heart, its roles in normal and abnormal physiology in other tissues could be explored. Answering all of these questions will hopefully bring us closer to the development of a new drug, which could inhibit MG23 to some degree, and perhaps reduce the cardiotoxicity effects that some patients treated with DOX unfortunately suffer.

| | | SP | | |
|-------------|-----|--|----------------|-----|
| TM109_HUMAN | 1 | MAASSISSFPWGKHFKAILMVLVALILLHSALAQSRDFAPPGQQKREAPVDVLTQIGRS | | 60 |
| TM109_MOUSE | 1 | MAGAHSTPLWSRHLKAVLMVLVALFLVHSASAQSHREFASPGQQKETSADILTQIGRS | | 60 |
| | | ***: : *.:*: | | |
| | | TM1 | | |
| TM109_HUMAN | 61 | VRGTLDAWIGPETMHLVSESSQVLWAISSAISVAFFALSGIAAQLLNALGLAGDYLAQG | | 120 |
| TM109_MOUSE | 61 | LKEMLDTWLGPETMHVISETLLQVMWAISSAISVA C FALSGIAAQLLSALGLDGEQLTQG | | 120 |
| | | :: **: | | |
| | | TM2 | | |
| TM109_HUMAN | 121 | LKLSPGQVQTFLLWGAGALVYVWLLSLLGLVLALLGRILWGLKLVIFLAGFVALMRSVP | | 180 |
| TM109_MOUSE | 121 | LKLSPSQVQVQTFLLWGAAALVIYWLLSLLGLVLALLGRILGGLKLVLFVAGFVALVRSVP | | 180 |
| | | *****.*: | | |
| | | TM3 | | |
| TM109_HUMAN | 181 | DPSTRALLLLALLLYALLSRLTGSRSASGAQLEAKVRGLERQVEELRWRQRAAKGARSV | | 240 |
| TM109_MOUSE | 181 | DPSTRALMLLALLTLFALLSRLTGSRSSGSHLEAKVRGLERQIEELRGRQRAAKMPRSM | | 240 |
| | | *****.*: | | |
| TM109_HUMAN | 241 | EEE | Identity 75.3% | 243 |
| TM109_MOUSE | 241 | EEE | Similar 92.2% | 243 |
| | | *** | | |

Figure 8 – Aligned amino acid sequences of human and mouse MG23, also known as TMEM109, with the described cysteine residue circled. Figure produced using EMBEL-EBI LALIGN. (Unpublished data Pitt lab)

Acknowledgements

I would like to give thanks to the entire Laidlaw foundation for support throughout the project, and also to the Laidlaw scholars whose matched experiences made the journey even more enjoyable. Crucially, I would like to thank Dr Sam Pitt, Quenton Hurst, Dr Amy

Dorward, Jordan Marsh, and Katie Abraham for all their help and guidance throughout and beyond the 6 weeks of this project.

References

1. Johnson-Arbor K, Dubey R. Doxorubicin. *StatPearls*. StatPearls Publishing Copyright © 2022, StatPearls Publishing LLC.; 2022.
2. Mitry MA, Edwards JG. Doxorubicin induced heart failure: Phenotype and molecular mechanisms. *Int J Cardiol Heart Vasc*. Mar 2016;10:17-24. doi:10.1016/j.ijcha.2015.11.004
3. Nitiss JL. DNA topoisomerase II and its growing repertoire of biological functions. *Nature Reviews Cancer*. 2009/05/01 2009;9(5):327-337. doi:10.1038/nrc2608
4. Chen T, Sun Y, Ji P, Kopetz S, Zhang W. Topoisomerase II α in chromosome instability and personalized cancer therapy. *Oncogene*. 2015/07/01 2015;34(31):4019-4031. doi:10.1038/onc.2014.332
5. Kalyanaraman B. Teaching the basics of the mechanism of doxorubicin-induced cardiotoxicity: Have we been barking up the wrong tree? *Redox Biol*. Jan 2020;29:101394. doi:10.1016/j.redox.2019.101394
6. Chatterjee K, Zhang J, Honbo N, Karlner JS. Doxorubicin cardiomyopathy. *Cardiology*. 2010;115(2):155-62. doi:10.1159/000265166
7. Wang Q, Michalak M. Calsequestrin. Structure, function, and evolution. *Cell Calcium*. Sep 2020;90:102242. doi:10.1016/j.ceca.2020.102242
8. Fearnley CJ, Roderick HL, Bootman MD. Calcium signaling in cardiac myocytes. *Cold Spring Harb Perspect Biol*. Nov 1 2011;3(11):a004242. doi:10.1101/cshperspect.a004242
9. Guo W, Sun B, Xiao Z, et al. The EF-hand Ca²⁺ Binding Domain Is Not Required for Cytosolic Ca²⁺ Activation of the Cardiac Ryanodine Receptor. *J Biol Chem*. Jan 29 2016;291(5):2150-60. doi:10.1074/jbc.M115.693325
10. MacLennan DH, Chen SR. Store overload-induced Ca²⁺ release as a triggering mechanism for CPVT and MH episodes caused by mutations in RYR and CASQ genes. *J Physiol*. Jul 1 2009;587(Pt 13):3113-5. doi:10.1113/jphysiol.2009.172155
11. Intracellular calcium release and cardiac disease - PubMed. <https://pubmed.ncbi.nlm.nih.gov/15709953/>
12. Mitsugumin 23 Forms a Massive Bowl-Shaped Assembly and Cation-Conducting Channel | Biochemistry. <https://pubs.acs.org/doi/full/10.1021/bi1019447>
13. Bers DM. Cardiac Sarcoplasmic Reticulum Calcium Leak: Basis and Roles in Cardiac Dysfunction. *Annual Review of Physiology*. 2014;76(1):107-127. doi:10.1146/annurev-physiol-020911-153308
14. Pinton P, Giorgi C, Siviero R, Zecchini E, Rizzuto R. Calcium and apoptosis: ER-mitochondria Ca²⁺ transfer in the control of apoptosis. *Oncogene*. Oct 27 2008;27(50):6407-18. doi:10.1038/onc.2008.308
15. Thompson CB. Apoptosis in the pathogenesis and treatment of disease. *Science*. Mar 10 1995;267(5203):1456-62. doi:10.1126/science.7878464
16. Kim H-E, Du F, Fang M, Wang X. Formation of apoptosome is initiated by cytochrome c-induced dATP hydrolysis and subsequent nucleotide exchange on Apaf-1. *Proceedings of the National Academy of Sciences*. 2005;102(49):17545-17550. doi:doi:10.1073/pnas.0507900102

17. Bauer TM, Murphy E. Role of Mitochondrial Calcium and the Permeability Transition Pore in Regulating Cell Death. *Circ Res*. Jan 17 2020;126(2):280-293. doi:10.1161/circresaha.119.316306
18. Yamazaki T, Sasaki N, Nishi M, Takeshima H. Facilitation of DNA damage-induced apoptosis by endoplasmic reticulum protein mitsugumin23. *Biochem Biophys Res Commun*. Feb 5 2010;392(2):196-200. doi:10.1016/j.bbrc.2010.01.013
19. Bovo E, Mazurek SR, Blatter LA, Zima AV. Regulation of sarcoplasmic reticulum Ca²⁺ leak by cytosolic Ca²⁺ in rabbit ventricular myocytes. *J Physiol*. Dec 15 2011;589(Pt 24):6039-50. doi:10.1113/jphysiol.2011.214171
20. Walker Mark A, Williams George SB, Kohl T, et al. Superresolution Modeling of Calcium Release in the Heart. *Biophysical Journal*. 2014;107(12):3018-3029. doi:10.1016/j.bpj.2014.11.003
21. Zima AV, Bovo E, Bers DM, Blatter LA. Ca²⁺ spark-dependent and -independent sarcoplasmic reticulum Ca²⁺ leak in normal and failing rabbit ventricular myocytes. *J Physiol*. Dec 1 2010;588(Pt 23):4743-57. doi:10.1113/jphysiol.2010.197913
22. Marx SO, Reiken S, Hisamatsu Y, et al. PKA phosphorylation dissociates FKBP12.6 from the calcium release channel (ryanodine receptor): defective regulation in failing hearts. *Cell*. May 12 2000;101(4):365-76. doi:10.1016/s0092-8674(00)80847-8
23. Reilly-O'Donnell B, Robertson GB, Karumbi A, et al. Dysregulated Zn(2+) homeostasis impairs cardiac type-2 ryanodine receptor and mitsugumin 23 functions, leading to sarcoplasmic reticulum Ca(2+) leakage. *J Biol Chem*. Aug 11 2017;292(32):13361-13373. doi:10.1074/jbc.M117.781708
24. Sitsapesan R, Montgomery RA, MacLeod KT, Williams AJ. Sheep cardiac sarcoplasmic reticulum calcium-release channels: modification of conductance and gating by temperature. *J Physiol*. Mar 1991;434:469-88. doi:10.1113/jphysiol.1991.sp018481
25. Venturi E, Mio K, Nishi M, et al. Mitsugumin 23 forms a massive bowl-shaped assembly and cation-conducting channel. *Biochemistry*. Apr 5 2011;50(13):2623-32. doi:10.1021/bi1019447
26. Bernuzzi F, Recalcati S, Alberghini A, Cairo G. Reactive oxygen species-independent apoptosis in doxorubicin-treated H9c2 cardiomyocytes: role for heme oxygenase-1 down-modulation. *Chem Biol Interact*. Jan 15 2009;177(1):12-20. doi:10.1016/j.cbi.2008.09.012
27. Ackers-Johnson M, Li PY, Holmes AP, O'Brien SM, Pavlovic D, Foo RS. A Simplified, Langendorff-Free Method for Concomitant Isolation of Viable Cardiac Myocytes and Nonmyocytes From the Adult Mouse Heart. *Circ Res*. Sep 30 2016;119(8):909-20. doi:10.1161/circresaha.116.309202
28. Park S. Mechanical Alteration Associated With Chemotherapeutic Resistance of Breast Cancer Cells. *J Cancer Prev*. Jun 2018;23(2):87-92. doi:10.15430/jcp.2018.23.2.87
29. Antonucci S, Di Sante M, Tonolo F, et al. The Determining Role of Mitochondrial Reactive Oxygen Species Generation and Monoamine Oxidase Activity in Doxorubicin-Induced Cardiotoxicity. *Antioxid Redox Signal*. Mar 1 2021;34(7):531-550. doi:10.1089/ars.2019.7929
30. Pecoraro M, Rodríguez-Sinovas A, Marzocco S, et al. Cardiotoxic Effects of Short-Term Doxorubicin Administration: Involvement of Connexin 43 in Calcium Impairment. *Int J Mol Sci*. Oct 11 2017;18(10)doi:10.3390/ijms18102121